JOURNAL OF CATALYSIS 130, 238–256 (1991)

Surface Structure and Reactivity of V–Ti–O Catalysts Prepared by Solid-State Reaction

2. Nature of the Active Phase Formed during *o*-Xylene Oxidation

G. CENTI,* D. PINELLI,* F. TRIFIRÓ,* D. GHOUSSOUB,† M. GUELTON,† AND L. GENGEMBRE†

Department of Industrial Chemistry and Materials, V.le Risorgimento 4, 40136 Bologna, Italy; and Lab. de Catalyse Hétérogène et Homogène URA CNRS 402, Univ. Sciences et Techniques de Lille Flandres-Artois, Villeneuve d'Ascq Cedex, France

Received May 9, 1990; revised January 21, 1991

The modifications occurring to V_2O_5 crystallites supported on TiO_2 (anatase or rutile) in contact with an *o*-xylene/air flow at about 600 K are characterized by determining the change in the valence state of vanadium through chemical analyses, the variation in the vanadium coordination environment through FT–IR and solid-state ^{51}V NMR spectroscopies, and the modification in the nature and distribution of the vanadium-oxide phase by means of XRD and XPS analyses. Results are analyzed with reference to the time-on-stream modifications in the catalytic behavior in *o*-xylene oxidation to phthalic anhydride of these catalysts and to the catalytic behavior and physicochemical characteristics of V_3O_7 supported on TiO_2 and of an unsupported partially reduced vanadium-oxide phase. On anatase samples, the TiO_2 surface is covered homogeneously by a V^{IV}–V^{V} partially hydrated mono- or bilayer. Overlaying this phase a hydrated V_3O_7-like phase (V^{V} : V^{IV} ratio of about 2 : 1) is also present as amorphous multilayer patches. In rutile samples, the former phase is no longer present, but instead islands of partially oxidized V_2O_4 are found together with the same partially reduced V-oxide phase as in the anatase samples. Catalytic results indicate that both phases have roughly similar catalytic behaviors and that the role of the TiO_2 support both in the anatase and rutile forms is to increase the number of surface sites, but not to modify their nature which depends only on the modifications occurring during the catalytic tests.

INTRODUCTION

In spite of the great number of papers dealing with the subject (*1*, *2* and references therein) existing information on the structural model of the vanadium-oxide active phase on TiO_2 during the oxidation of *o*-xylene to phthalic anhydride is contradictory. In addition, few data are available on the *in situ* transformations during the catalytic tests and thus on the real nature of the active phase. Most of the authors discuss possible differences in the vanadium oxide on the anatase or rutile TiO_2 surfaces before the catalytic tests without characterizing the differences after interaction with the *o*-xylene/air reagent mixture (*3*, *4* and references therein), which is known to cause considerable modification of the surface structure of vanadium oxide (*5*).

The surface interaction of V_2O_5 with TiO_2 has been reported in a previous paper (*6*) dealing with the formation of V^{IV} in a layer on the titania surface which leads to considerable modification of its characteristics. This illustrates the necessity for a more detailed analysis of the structure of the active phase of these catalysts after long-term catalytic tests.

In this paper, the transformations that occur to the vanadium oxide with time-on-stream during the catalytic tests in *o*-xylene selective oxidation were analyzed. The study of these processes is fundamental for

0021-9517/91 $3.00

understanding the real nature of the active phase as well as for a correct analysis of the role of TiO_2.

The preparation method adopted in this study was solid-state reaction. As indicated also in the first part (*6*), this method is particularly suitable. It allows catalysts to be obtained that are comparable both in activity and selectivity to those prepared by usual wet impregnation methods or by grafting techniques, but has the advantage of much better identification of the starting situation for the analysis of the evolution of the catalytic behavior with time-on-stream and with the physicochemical transformation of the catalyst.

EXPERIMENTAL

Catalyst Preparation

Catalysts were prepared by solid-state reaction. V_2O_5 was gently mixed with TiO_2 either in the anatase or rutile crystalline forms, and successively calcined and treated *in situ* according to the method described in the first part (*6*). The anatase or rutile titanium oxide was prepared by hydrolysis of $TiCl_4$ and changing the pH of the solution before precipitation with an ammonia solution, as described previously (*7*). After drying the precipitate, the sample was calcined at 770 K. The final surface areas were 9.6 and 8.9 m^2/g for anatase and rutile TiO_2, respectively.

As shown in the previous paper (*6*) during calcination and consecutive catalytic tests in *o*-xylene oxidation, considerable amounts of V^{IV} form which modify the reactivity of the TiO_2 surface. This effect overlaps the modifications occurring in the V_2O_5 in contact with the *o*-xylene/air stream. In order to analyze this last effect better, the following procedure was adopted. Samples loaded with 7.7% (w/w) of V_2O_5 (a typical amount for industrial catalysts) were used in a long-term catalytic test (at least 500 h), unloaded, and washed with a diluted sulphuric acid solution to remove the *weakly interacting* vanadium oxide from the V^{IV}–TiO_2 surface, according to the procedure described in the first part (*6*). New catalysts were prepared by adding different amounts of crystalline V_2O_5 to this V^{IV}–TiO_2 residual powder. These catalysts are henceforward indicated with the label % A or % R, where A and R indicate the anatase or rutile form of TiO_2 and % indicates the amount, expressed as % (w/w), of the added V_2O_5 with respect to the total weight of the catalyst.

A V^{IV}–V^{V} mixed valence oxide catalyst (sample V) nonsupported on TiO_2 was prepared by dropping a solution of V^{IV}, obtained by dissolution and reduction with oxalic acid of V_2O_5, into an ammonia solution (pH = 9). The precipitate was dried at 350 K and calcined at 530 K. This method produces a vanadium oxide which exhibits an IR spectrum and a mean valence state of vanadium very similar to those of the vanadium oxide on the TiO_2 (*8*).

Finally, a sample was prepared by adding 5.05 wt% crystalline V_3O_7 to the V^{IV}–TiO_2 (anatase) powder. This catalyst is referred to as V_3O_7-A. The V_3O_7 was synthetized according to the method of Waltersson *et al.* (*9*) by a series of consecutive heat treatments under vacuum (773 K, 24 h) with intermediate grinding, starting from a mixture of crystalline V_2O_3 and V_2O_5, in the proportions necessary to obtain the mean vanadium valence of V_3O_7 (4.67). Identification of the phase as V_3O_7 was made by comparison of the X-ray diffraction (XRD) patterns.

Characterization

The catalysts were tested in a conventional laboratory apparatus with a tubular fixed-bed flow reactor working at atmospheric pressure, and on-line gas chromatographic analysis of reagent and product composition. The standard reactant composition was 1.5% *o*-xylene, 20% O_2, and the remainder helium. The catalyst (0.5 g) was loaded as grains (0.250–0.420 mm). A thermocouple, placed in the middle of the catalyst bed, was used to verify that the axial temperature profile was within 5 K. Further details on the apparatus used, the analytical procedure, and the verification of the ab-

sence of diffusional limitations on the reaction rates have been reported previously (*10*).

The chemical analysis procedure and the criteria for the classification of the vanadium species as soluble or *weakly interacting* and insoluble or *strongly interacting* are the same as those illustrated previously (*6*). The possible influence of the cooling procedure after catalytic tests on the valence state of vanadium was verified comparing the results of some samples adopting the following two procedures of cooling of V–Ti–O samples after catalytic tests: (i) quick cooling of the sample by extraction from the reactor (in air), (ii) slow cooling inside the reactor in a dried inert (N_2) flowing atmosphere. The equivalence of the results suggests that the cooling procedure does not affect the results obtained by chemical analysis. Normally the first procedure of cooling was then used.

X-ray diffraction patterns (powder technique) were obtained using Ni-filtered Cu$K\alpha$ radiation and a Philips computer controlled instrument.

Surface areas were determined using the BET method with nitrogen adsorption at 77 K and a Carlo Erba Sorptomatic instrument.

Wide-line solid-state vanadium nuclear magnetic resonance (^{51}V NMR) spectra were recorded using a CXP100 Bruker spectrometer at 26.289 MHz. The spectral width was 125 kHz. A 22.5° pulse angle (*11, 12*) and a 0.7-s repetition time were used. The spectra were obtained using quadrature detection from the accumulation of at least 40,000 transients. Differences between sample and probe free induction decays were calculated before exponential multiplication with 100 Hz line broadening. A special insert was used to allow measurements on vertical 10-mm o.d. Liquid $VOCl_3$ was chosen as a reference for chemical shifts ($\delta = 0$).

X-ray photoelectron spectroscopy (XPS) results were obtained using a LHS 10 spectrometer or a VG ESCALAB instrument equipped with an Al anode which was operated at 13 kV and 20 mA current emission ($h\nu = 1486.6$ eV). Binding energies were determined using the O_{1s} peak at 529.8 eV as a reference to correct the charge effect occurring on the sample which is mounted on an indium plate. The O_{1s} peak was used to correct the charge effect instead of C_{1s} peak, because, especially in the samples after the catalytic tests, the C_{1s} peak is very broad due to the presence of several partially overlapping peaks related to the presence of both contaminant molecules, and adsorbed species (especially aromatics) remained on the surface after the catalytic tests. Furthermore, XPS analysis of several pure mono- or polycrystalline V-oxides after various pretreatments indicates that O_{1s} peak is a more reliable reference than C_{1s} signal (*15*). The atomic ratios N_V/N_O and N_{Ti}/N_O were determined from the general relationship,

$$\frac{N_1}{N_2} = \frac{I_1}{I_2} \cdot \frac{\sigma_2}{\sigma_1} \cdot \frac{E_2}{E_1} \cdot \frac{E_2 + C}{E_1 + C} \cdot \frac{1 + \beta_2/4}{1 + \beta_1/4}$$

with the cross sections σ obtained from Scofield (*13*), the parameter of asymmetry β taken from Reilman *et al.* (*14*), E the experimental kinetic energy, C a constant taken equal to 100 eV (*15*), and I the area of the ($V_{2p\ 3/2} + V_{2p\ 1/2}$), of the O_{1s} or of the ($Ti_{2p\ 3/2} + Ti_{2p\ 1/2}$) peaks. The X-ray O_{1s} satellite was subtracted from the peaks of vanadium by deconvolution. The validity of the relationship was verified using pure oxide as reference samples. The sputtering of the surface was realized using a Ne^+ ion gun after calibration of the amount of layers removed with time (*15*). The sputtering yield for V is nearly equal to that of Ti and about 1.2 times larger than that of O. For the determination of depth profile a model of vanadia blocks of different thickness on the titania surface covered with a monolayer of vanadia was used (*15*). This model is in agreement with other XPS measurements on V–TiO_2 systems (*1* and reference therein).

Fourier transform–infrared (FT–IR) spectra were recorded using a Perkin–Elmer 7200 Fourier transform infrared spectrometer and the KBr disk technique. Cali-

brated amounts of V–Ti–O samples (around 0.1 wt% with respect to KBr) were used and electronically calibrated subtraction of the TiO_2 contribution to the spectrum was carried out.

RESULTS

Catalytic Tests

The catalytic behavior in *o*-xylene oxidation of two series of catalysts was analyzed as a function of time-on-stream. The catalysts were prepared by adding different amounts (from 0 to 5.05 wt%) of crystalline V_2O_5 to V^{IV}-modified TiO_2 either in the anatase or rutile forms. The V^{IV}–TiO_2 samples were prepared as described in the experimental part from catalysts after long-term catalytic test (at least 500 h). This allows an analysis of just the evolution of the V_2O_5 phase without the side reaction of formation of a strongly interacting (non-soluble) V^{IV} species as shown in the first part (*6*). This species, as previously described (*6*, *8*), can be distinguished from other V^{IV} species formed by reduction of V_2O_5 during catalytic tests because it cannot be extracted in dilute sulphuric acid or ammonia solutions.

The catalytic data of the anatase samples after at least 100 h of time-on-stream are reported in Fig. 1. Several indexes of activity (Fig. 1a) and of selectivity (Fig. 1b) are reported for a better analysis of the results. In particular, the temperature of 50% conversion and the conversion at two different temperatures are reported as indexes of activity. The maximum yield to phthalic anhydride (PA), the selectivity to PA at 50% and 95% of *o*-xylene conversion, and the selectivity to phthalide (PI) at 50% conversion are reported as indexes of selectivity. The phthalide is an intermediate in the *o*-xylene conversion to PA according to Scheme 1. Carbon oxides were the only other products detected.

For an equivalent conversion, an increase in the relative formation of phthalide with respect to phthalic anhydride may be assumed as an index of a lowering of the oxygen insertion properties of the catalyst.

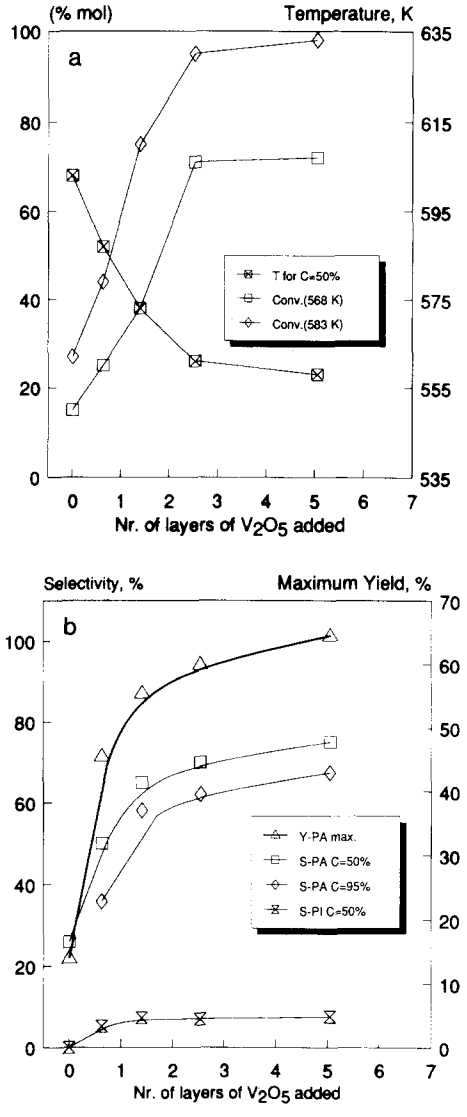

FIG. 1. Effect of the amount of V_2O_5 added to V^{IV}-modified TiO_2 anatase (see text) on the temperature of 50% conversion and on the conversion at two temperatures (a) and on the maximum yield (Y-max) of phthalic anhydride (PA), on the selectivity (*S*) to PA at 50% and 95% *o*-xylene conversion and on the selectivity to phthalimide (PI) at 50% conversion (b). Catalytic data refer to the steady-state catalytic behavior after at least 200 h of time-on-stream.

For the analysis of these data it should be taken into account that the V^{IV} species already present on the TiO_2 surface (see above) are active in *o*-xylene conversion to phthalic anhydride, even though these sam-

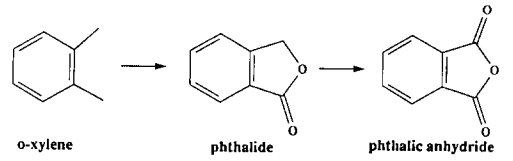

SCHEME 1. Reaction scheme for the synthesis of phthalic anhydride from *o*-xylene.

ples are less active and less selective than the normal V–Ti–O samples in which V^V species were not extracted by the washing procedure (*6*). Thus the addition of crystalline V_2O_5 results in an increase in the activity and in the selectivity. The activity increases linearly with increasing amounts of V_2O_5 up to a content corresponding to that necessary to cover the surface of the TiO_2 with two to three layers of oxide (one layer corresponds to about 1.0 wt% of V_2O_5 based on a surface area of about 10 m^2/g of the catalyst (*1*)). Further additions of V_2O_5 proved to have very little, if any, effect on the activity. The maximum yield to phthalic anhydride rises from 13 to 45 mol% as a consequence of the first V_2O_5 addition, then increases slowly and almost linearly with increasing V_2O_5 content up to the maximum value of 63% in the case of the 5.05% A catalyst (this amount corresponding to about five layers).

The catalytic data for the rutile samples after at least 100 h of time-on-stream are reported in Fig. 2 in a manner analogous to that described for the anatase samples. The catalyst without V_2O_5 added (0% R) is more active and selective in the oxidation of *o*-xylene than the corresponding anatase sample without V_2O_5 added (0% A), as discussed in the first part of the work (*6*). The activity increases with the first addition of V_2O_5 then remains practically constant with further additions in contrast to the results for the anatase samples. The maximum yield to PA increases with increasing vanadium oxide content while the selectivity shows a different trend at different conversions. At high conversion (C = 95%), the selectivity increases almost linearly with the amount of V_2O_5 added. On the other hand, at lower conversion (C = 50%), the selectivity is maximum in the sample without added V_2O_5 and decreases linearly with increasing

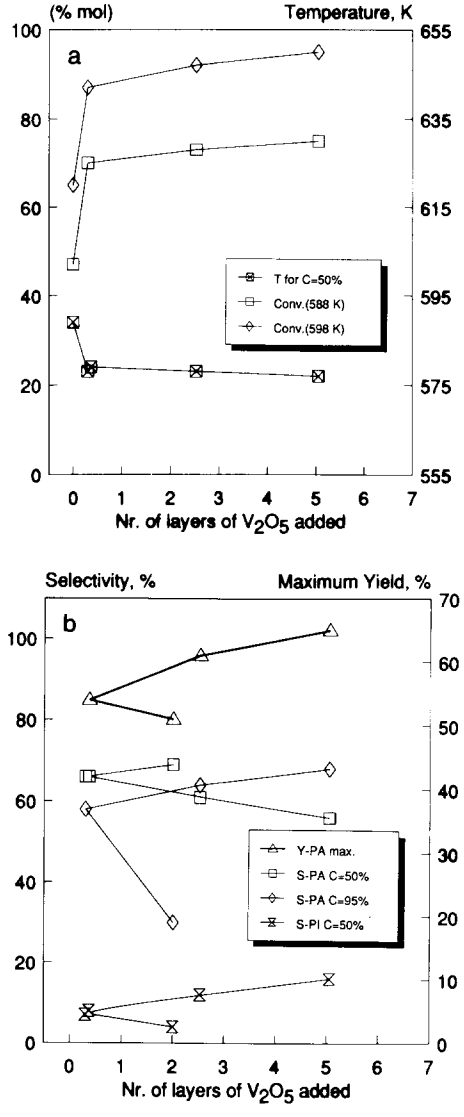

FIG. 2. Effect of the amount of V_2O_5 added to V^{IV}-modified TiO_2 rutile (see text) on the temperature of 50% conversion and on the conversion at two temperatures (a) and on the maximum yield (Y-max) of phthalic anhydride (PA), on the selectivity (S) to PA at 50% and 95% *o*-xylene conversion and on the selectivity to phthalimide (PI) at 50% conversion (b). Catalytic data refer to the steady-state catalytic behavior after at least 200 h of time-on-stream.

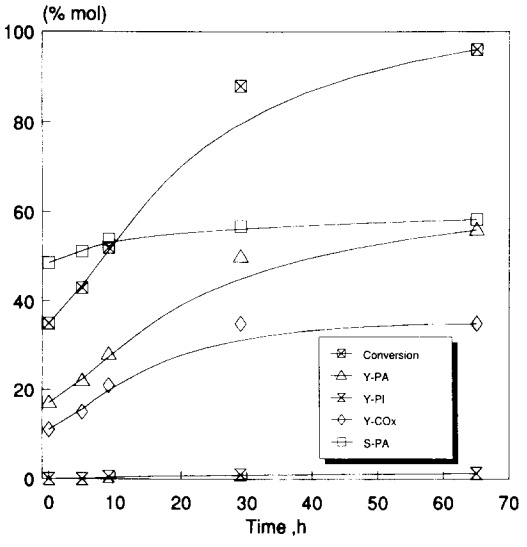

FIG. 3. Change in the catalytic behavior at 597 K of a 2.53% A sample as a function of time on stream during *o*-xylene oxidation to phthalic anhydride. Symbols: *Y* yield, *S* selectivity, PA phthalic anhydride, PI phthalimide, CO_x carbon oxides.

amounts of soluble vanadium oxide. This difference in the behavior at different conversions is mainly due to the formation of phthalide. At high conversion the amount of PI is negligible.

The time-on-stream evolution of an anatase and a rutile sample is reported in Figs. 3 and 4, respectively, in order to show the change of the catalytic behavior during *o*-xylene oxidation. The nature of the process is nearly the same in all the other samples and does not depend greatly on the amount of V_2O_5 added. The activity and the selectivity increases in all the samples, with the exception of the 0% A sample. It is important to note that, as reported previously (*6*), the 0% R sample evolves in time (this fact is testimony to a transformation of the surface), while the 0% A sample does not evolve, because surface V^{IV} species on TiO_2 (anatase) are stable in the reaction medium (*6*).

Moreover, during the catalytic tests, an important difference in the rate of transformation of the catalysts was observed between the anatase and the rutile samples. The rate for anatase samples is about twice that of corresponding rutile sample and thus the time to reach the steady state in the catalytic performance of rutile samples is longer.

The steady-state catalytic behavior of an unsupported mixed valance vanadium catalyst is reported in Fig. 5. Even though the amount of vanadium utilized in the catalytic tests is about 10 times higher than that of vanadium oxide in the $V–TiO_2$ catalyst, the activity of this unsupported catalyst is still lower. The selectivity to PA, however, is very high and very comparable to that of $V–TiO_2$ catalysts. This indicates that the main difference between supported and unsupported vanadium oxide is in the specific activity per gram of the active vanadium oxide component, but not in the selective behavior. The production of phthalide is slightly higher than that of $V–TiO_2$ anatase catalysts but lower than that of the $V–TiO_2$ rutile samples. This catalyst rapidly (about 4 h) reaches a steady-state catalytic behavior.

The steady-state catalytic behavior of the

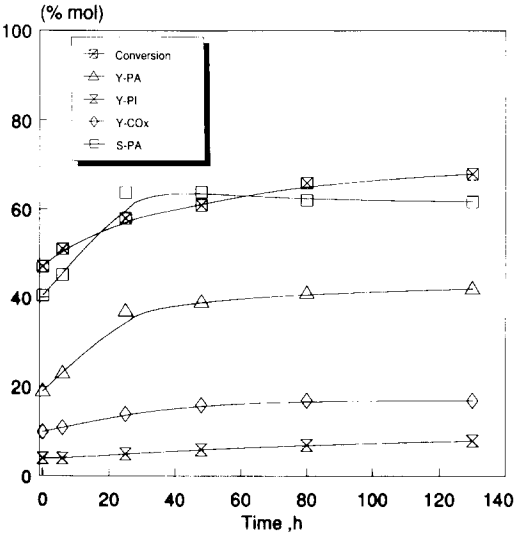

FIG. 4. Change in the catalytic behavior at 597 K of a 5.05% R sample as a function of time-on-stream during *o*-xylene oxidation to phthalic anhydride. Symbols as in Fig. 3.

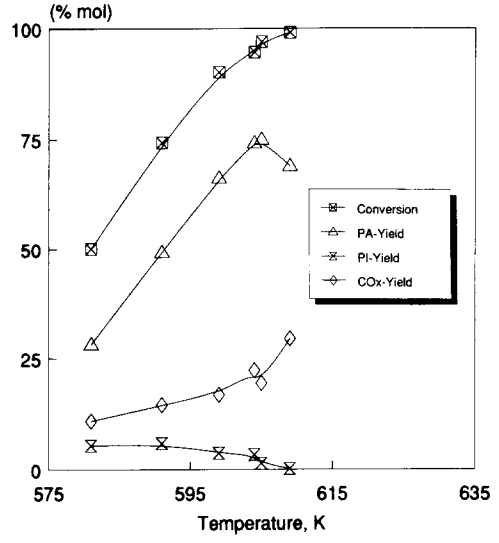

FIG. 5. Steady-state catalytic behavior (after 4 h) of a mixed valence unsupported sample of vanadium oxide (sample V—see text). Symbols as in Fig. 3.

catalyst prepared by solid-state interaction between crystalline V_3O_7 and TiO_2 anatase is reported in Fig. 6. The catalyst is not very active and selective in the first hours of reaction, but both activity and selectivity

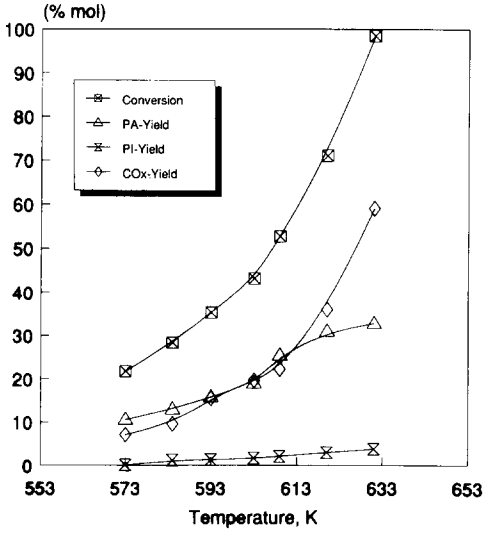

FIG. 6. Steady-state catalytic behavior (after 24 h) of a sample of 5.05% (w/w) V_3O_7 on TiO_2 (anatase). Symbols as in Fig. 3.

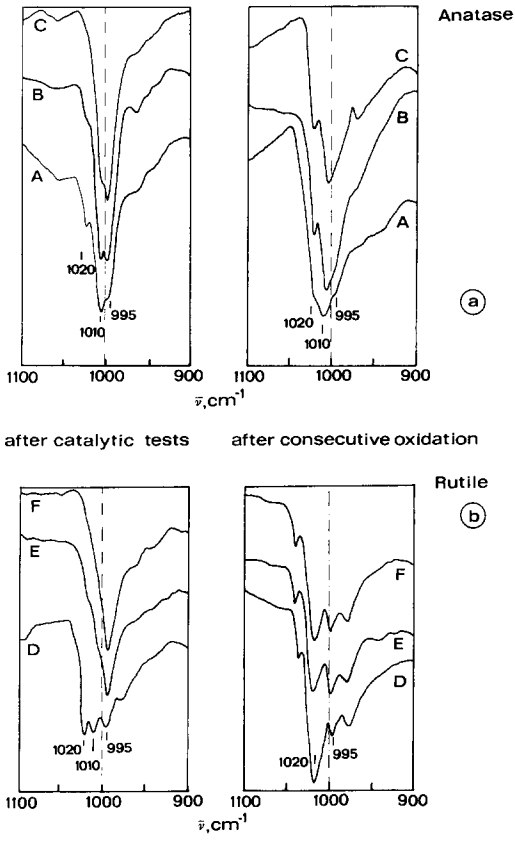

FIG. 7. FT–IR spectra in the νV=O region of 5.05% (w/w) V_2O_5 on TiO_2 (Fig. 7a on TiO_2 anatase; Fig. 7b on TiO_2 rutile) samples after different time-on-stream during *o*-xylene oxidation and after consecutive calcination (673 K, 3 h). Figure 7a: (A) after 13 h, (B) after 40 h, (C) after 65 h. Figure 7b: (D) after 24 h, (E) after 80 h, (F) after 135 h.

rapidly increase with time-on-stream as for V_2O_5–TiO_2 samples (see Fig. 3). However, the attainment of the steady-state activity is much more rapid and after about 20 h a constant catalytic behavior is observed. The final results (Fig. 6) are very comparable to those of the 5.05% A sample.

Fourier Transform–Infrared (FT–IR) and Chemical Analysis Characterization

The FT–IR spectra in the νV=O region of the 5.05% samples as a function of time-on-stream in contact with *o*-xylene/air flow (568 K) are reported in Fig. 7 together with

TABLE 1

Mean Valence State of Vanadium (±0.05) in the Vanadium Oxide Extracted by a Dilute H_2SO_4 Solution (See Text) for 5.05% (w/w) V_2O_5 on TiO_2 after Different Time-on-Stream during *o*-Xylene Oxidation and after Consecutive Calcination (673 K, 3 h)

Type of TiO_2	Time-on-stream (h)	Sample (Fig. 7)	Mean valence state	
			After catalytic tests	After consecutive tests
Anatase	13	A	4.81	4.95
	40	B	4.72	4.91
	65	C	4.71	4.89
Rutile	24	D	4.86	4.97
	80	E	4.77	4.93
	135	F	4.72	4.92

the FT–IR spectra of the corresponding sample after consecutive calcination (673 K, 3 h). The corresponding mean valence state of vanadium in the fraction extracted by a dilute sulphuric acid solution (*6*) is reported in Table 1. At the steady-state catalytic behavior both on anatase and rutile samples (Figs. 7B, 7C, and 7E, 7F) the crystalline V_2O_5 (characterized by a sharp main band at 1022 cm^{-1}-ν_sV=O with a small shoulder at 980 cm^{-1}-ν_{as}V=O) is transformed to a phase characterized by a sharp band centered at 995 cm^{-1} and by a mean valence state of about 4.7. X-ray diffraction analysis of the samples indicates a parallel disappearance of the crystalline V_2O_5 and formation of an amorphous vanadium oxide phase. The shifting to lower frequencies of the stretching frequency of the V=O double bond may be attributed to two parallel effects, the first due to a change from the highly distorted pseudo-pyramidal coordination of vanadium in the V_2O_5 to nearly octahedral coordination (due to structural transformation and to the coordinatively adsorbed water) and the second to the electronic effect due to the presence of neighboring V^{4+} sites.

No remarkable differences in the IR spectra and mean valence state can be observed in the anatase and rutile samples after attainment of steady-state catalytic behavior, but a different rate of evolution with time-on-stream is shown. The 1022 cm^{-1} IR band (V_2O_5) transforms progressively to the band centered at 995 cm^{-1} (reduced vanadium oxide after *o*-xylene oxidation) through the apparent intermediate formation of a phase characterized by a sharp band centered at about 1010 cm^{-1} and a higher mean valence state. From the comparison of the corresponding spectra for anatase and rutile samples (Fig. 7) it is evident that the slower rate of transformation to the reduced phase concerns the latter catalysts.

The tests of consecutive oxidation of these samples provide information about the stability of the reduced vanadium oxide phases formed to consecutive oxidation and thus are indicative of possible differences in the properties. FT–IR spectra (Fig. 7) and chemical analyses (Table 1) show that the stability of the reduced vanadium oxide phases to reform V_2O_5 crystallites is higher on TiO_2 anatase than on TiO_2 rutile.

The FT–IR spectra and the chemical analysis data of the mixed valence unsupported vanadium oxide (sample V), before and after the catalytic test are reported in Fig. 8. Before the catalytic test (spectrum *a*), a broadband centered at 980 cm^{-1} is present together with some broadbands at lower frequencies due to V–O–V bending. In samples supported on TiO_2, the IR region below 900 cm^{-1} cannot be analyzed due to overlap-

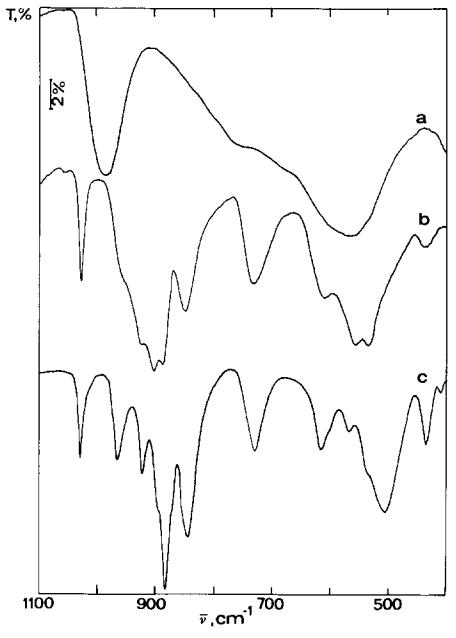

FIG. 8. FT–IR spectra of sample V (unsupported mixed valence vanadium oxide) before (a) and (b) after catalytic tests in *o*-xylene oxidation and of a sample of crystalline V_3O_7 (c). Mean valence state of vanadium as determined by chemical analysis: (a) 4.76, (b) 4.72, (c) 4.70.

ping of the more intense TiO_2 bands. After the catalytic test (spectrum *b*), the mean valence of the soluble vanadium oxide fraction is only slightly changed while the IR spectrum of the discharged sample is completely different and corresponds approximately to that of crystalline V_3O_7 (spectrum *c*).

The V_3O_7-A sample, on the contrary, shows a different evolution with time-on-stream (Fig. 9). Before the catalytic tests (spectrum *a*), the characteristic bands of V_3O_7 are visible. In particular, a sharp band is present at 1028 cm^{-1}. The shifting to higher frequency of the $\nu V{=}O$ symmetric stretching frequency with respect to corresponding band in V_2O_5 (1022 cm^{-1}), notwithstanding the V=O distance in V_3O_7 (1.62 Å) (*9*) is longer than in V_2O_5 (1.58 Å) (*16*), is probably connected to the different coupling of the symmetric and asymmetric $\nu V{=}O$ modes in the two structures, in agreement also with the splitting between the two bands. After the catalytic tests (spectrum *b*), considerable broadening of the spectrum is observed. The band at 1028 cm^{-1}, in particular, decreases considerably in intensity and a new band appears at 995 cm^{-1} indicating the formation of a phase similar to that formed in V_2O_5–TiO_2 samples after long-term catalytic tests (Fig. 7). The chemical analysis data show that the mean valence of soluble vanadia does not change significantly.

Wide-Line Solid-State ^{51}V NMR Spectra

The ^{51}V isotope (spin $\frac{7}{2}$) possesses a nuclear electric quadrupole moment and therefore its NMR spectrum is affected in the solid state by the interaction of this moment with electrostatic field gradients created by asymmetric electronic environments. The static NMR lineshape, dominated by chemical shift anisotropy related to the three principal components of the nuclei magnetic shielding tensor, gives more reliable information to differentiate between the various coordination environments of vanadium than does analysis of the isotropic chemical shift alone (*17–22*). The comparison of

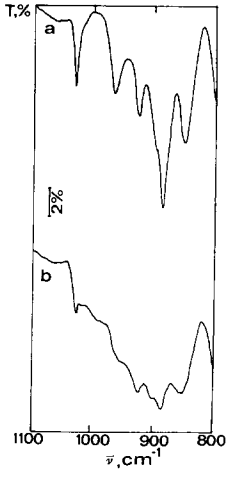

FIG. 9. FT–IR spectra of 5.05% (w/w) V_3O_7 on TiO_2 (anatase) before (a) and after (b) catalytic tests in *o*-xylene oxidation.

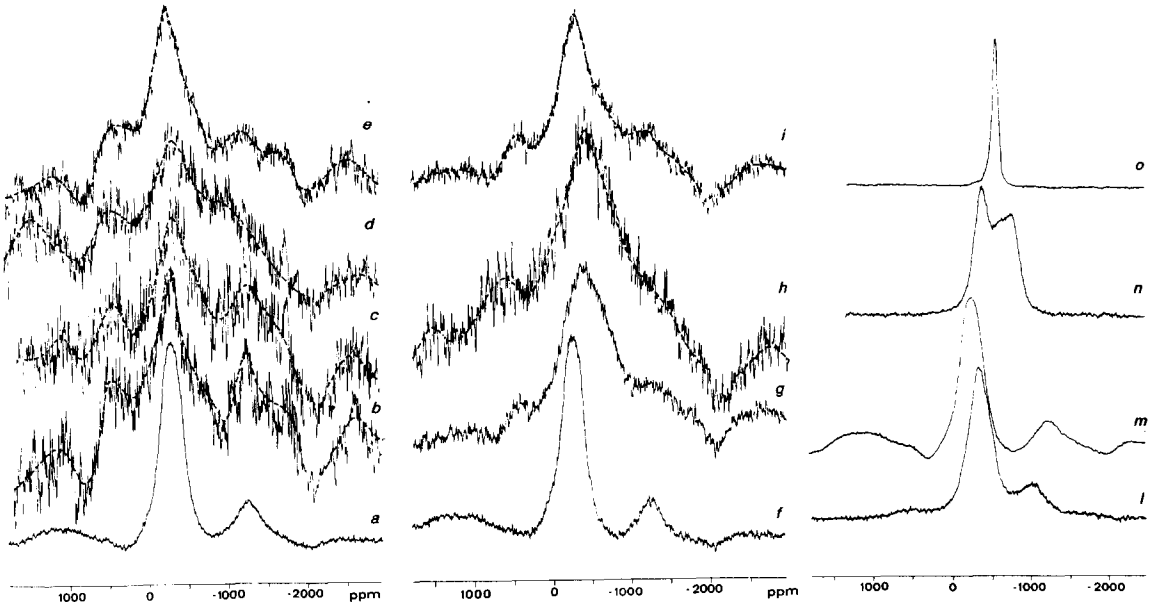

FIG. 10. Wide-line solid-state ^{51}V NMR spectra of 5.05% V_2O_5 on TiO_2 anatase (spectra *a* → *e*) and of 5.05% V_2O_5 on TiO_2 rutile (spectra *f* → *i*) after different treatments: *a* and *f* after calcination; *b*, *c*, and *d* after 24 h, 48 h, and 65 hours of time-on-stream in *o*-xylene oxidation, respectively; *g* and *h* after 40 h and 130 h of time-on-stream in *o*-xylene oxidation, respectively; *e* and *i*, samples d and h after consecutive calcination (773 K, 3 h). Spectra of reference compounds: *l*, hydrated gel of V_2O_5; *m*, sample *l* after calcination (773 K, 24 h); *n*, NH_4VO_3; *o*, K_3VO_4.

wide-line solid-state ^{51}V NMR spectra with selected chemical reference compounds can thus be usefully utilized for the study of the local coordination of V^V species on an oxide matrix. The ^{51}V NMR spectra and parameters of various model compounds with well-defined coordination environments have been previously reported (*17, 19, 21*). However, since the spectra are affected by the field strength and the impulse sequence, in this work the spectra of some selected reference compounds are also reported in order to facilitate comparison and analysis of the results (Fig. 10, spectra *l–o*).

The ^{51}V NMR spectra of V_2O_5 show a marked asymmetry of the central component (which is often the only visible transition in FT-NMR of powders) of the seven-line quadrupole pattern (*23, 24*); this asymmetry is due to anisotropic magnetic shielding deriving from the nearly fivefold coordination of the four equivalent vanadium sites in V_2O_5 [very distorted octahedron with one short V—O bond (1.58 Å, corresponding to a vanadium–oxygen double bond) and one very long V—O bond (2.78 Å)]. This coordination gives a nearly axially symmetric chemical shift tensor with maximized shielding along the axial direction.

The spectra of the dried and calcined (770 K) V_2O_5 samples prepared by precipitation (spectra *l* and *m*, respectively) are reported in Fig. 10. In the calcined sample (spectrum *m*), a central line is present at −320 ppm with a smaller line at −1280 ppm due to chemical shift anisotropy. Very small broad satellites at about 1000 ppm and −2100 ppm correspond to the first-order quadrupolar splitting. In the sample before calcination (spectrum *l*), the main line shifts at −361 ppm; the axial shielding resonance shift at −1050 ppm. The difference between the two spectra can be interpreted in terms of

change from a slightly distorted octahedral coordination of vanadium in the dried sample (according to the spectra of octahedral vanadium pyrovanadate compounds (*17, 19*)) to the nearly fivefold coordination typical of calcined V_2O_5. This is in agreement with the change in axial distortion observed by IR spectroscopy after heat treatments of V_2O_5 with a shift of $\nu V{=}O$ to higher frequencies (*25*). The reference spectra of NH_4VO_3 and of K_3VO_4 (spectra *n* and *o*, respectively) are indicative of tetrahedrally coordinated vanadium in metavanadate and *o*-vanadate, respectively, in which the electric field gradient changes from highly asymmetric (ammonium metavanadate where chains of vanadate groups are interconnected by two edges) to highly symmetric (potassium orthovanadate, where isolated monomeric vanadate groups are present). In these conditions, the quadrupolar frequency ν_Q is high in NH_4VO_3 and the second-order quadrupolar splitting of the central component appears as an asymmetric doublet in the powder spectrum (*11*).

On the basis of these indications the ^{51}V NMR spectra of V-oxide on anatase (spectra *a–e*) or on rutile TiO_2 (spectra *f–i*) can be analyzed. The spectra *a* and *f* refer to the samples after calcination, whereas the spectra *b–d* and *g–h* refer to the samples after different time on stream during *o*-xylene oxidation. The spectra *e* and *i* refer to the spectra of the *d* and *h* samples, respectively, after consecutive calcination (670 K, 3 h) in order to analyze the stability of the reduced vanadium-oxide species toward consecutive oxidation.

After calcination the spectra of vanadium oxide on TiO_2 anatase (a) or on rutile (f) indicate the presence of only V_2O_5, whereas a drastic modification is noted in all the samples after contact with the *o*-xylene/air stream. The following main features were observed: (i) the appearance of a resonance peak centered at around 500 ppm, (ii) a slight shift (around 50 ppm) in the position of the main peak with considerable line broadening of the spectra, (iii) a considerable decrease in the intensity of the spectra as shown by the increase in the noise/signal ratio.

The signal at about 500 ppm is typical of all partially reduced vanadium samples and can be attributed to the presence of V^{5+}—O—V^{4+} sites (*26*). The evolution with time-on-stream of the anatase samples (spectra *b–d*) indicates a progressive broadening of the spectra and a progressive narrowing of the chemical shift anisotropy with a shift in the parallel component from about -1300 ppm to about -1000 ppm. A slight shift in the position of the main peak (from -300 to about -350 ppm) is also observed. The spectra can be interpreted, on the basis of the previous discussion of the V_2O_5 spectra, as a progressive change with time-on-stream from a nearly square-pyramidal coordination such as in crystalline calcined V_2O_5 to an octahedral coordination such as in hydrated V_2O_5. The spectra, on the contrary, do not provide evidence, at least for the main species, of the presence of tetrahedrally coordinated vanadium. In addition, spectrum *d* agrees with that found by Eckert and Wachs (*17*) for vanadium oxide supported on anatase catalysts prepared by wet impregnation, and also attributed mainly to an octahedral coordination environment. This indicates the relative analogy of the coordination of V^{5+} sites in the sample after catalytic tests (spectrum *d*) or before the tests (*17*) using a suitable preparation procedure. The concentration of V^{V} species progressively decreases with time-on-stream as shown by the increase in the noise to signal ratio, due to the formation of an important amount of V^{IV}.

Under vacuum the coordination of vanadium species on an oxide support may change (*17, 21, 22*) as a consequence of the loss of coordination water. However, the relatively high partial pressure of water during the catalytic tests as well as the beneficial effect of steam addition on the selectivity in phthalic anhydride from *o*-xylene, indicate that during catalytic tests vanadium sites are in the hydrated form. The spectra

of the samples after evacuation treatment were thus considered not representative of the real situation of the vanadium sites during the catalytic reaction.

After consecutive oxidation of sample *d* (spectrum *e*) (i) the intensity of the signal increases, (ii) the main peak becomes narrower, and (iii) the chemical shift anisotropy increases, indicating a progressive change to reform the nearly fivefold coordination.

Similar spectra are observed in the rutile samples (spectra *g–i*). The intensity of the signal, however, is generally slightly higher as shown by the lower noise in the spectra, in agreement with the generally higher mean valence state of these samples after catalytic tests (Table 1). A slight shift in the peak maxima (spectra *g–h*) and relatively broader peaks compared to corresponding anatase samples (spectra *b–d*) could also be noted. These effects may be tentatively attributed to the presence in rutile samples of an additional species of V^V in a slightly different environment, in agreement with the possible partial oxidation in rutile samples of nonsoluble V^{IV} species to V^V (*6*). However, the difference observed in the peak shape do not allow a unique interpretation. The evolution of the spectra with time-on-stream or after consecutive oxidation is in line with that discussed for the anatase samples, but indicates the slower rate of transformation of vanadium oxide in rutile samples in comparison to anatase samples.

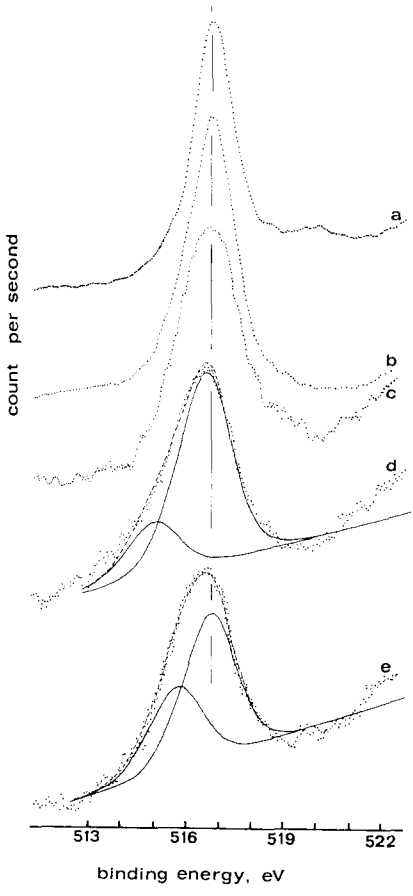

FIG. 11. X-ray photoelectron spectra (XPS) in the V_{2p} region of (a) V_2O_5, (b) a mechanical mixture of 5% (w/w) V_2O_5 and TiO_2, (c) a 9% (w/w) V-oxide on a high surface area (90 m^2/g) TiO_2 anatase-sample prepared by impregnation, (d) sample b after calcination (773 K, 24 h), (e) sample d after catalytic tests in *o*-xylene oxidation (at least 500 h of time-on-stream).

X-Ray Photoelectron Spectroscopy (XPS)

The XPS spectra in the $V_{2p\ 3/2}$ region of some V-oxide samples are reported in Fig. 11. The spectra have been corrected for sample charging effects using the O_{1s} peak as a reference. The O_{1s} X-ray satellite (11% of the intensity of the main O_{1s} peak) which partially overlaps the V_{2p} peaks was subtracted electronically.

The spectrum of V_2O_5 (spectrum *a*) shows the typical signal of V^V centered at 517.0 eV with a full width at half maximum (FWHM) of 1.4 eV. In a sample prepared from a mechanical mixture of V_2O_5 and TiO_2 (5% (w/w) of V_2O_5) the signal remains unchanged (spectrum *b*). Further calcination of this sample (spectrum *d*) produces a small shift (about 0.1 eV) in the peak position, but especially a strong broadening of the signal (FWHM of 2.0 eV) with an asymmetric tail on the lower binding energies side. The analysis of a sample (spectrum *c*) prepared by wet impregnation on a high surface area TiO_2 also shows a broadening of the spectrum (FWHM of 1.8 eV), but not the asymmetric tail. The amount of vanadium oxide in this sample, due to the high TiO_2 surface

TABLE 2

Values of the V/O, Ti/O, and V/Ti Atomic Ratios in VTiO Samples as Determined in XPS Measurements

Sample	Reference to Fig. 11	Surface area (m^2/g)	Atomic ratio		
			V/O	Ti/O	V/Ti
5% A					
After catalytic tests	e	9.8	0.129	0.281	0.459
and consecutive extraction	—	9.8	0.020	0.461	0.043
Mechanical mixture of 5% V_2O_5 and TiO_2 anatase	b	9.8	0.101	0.342	0.295
9% V_2O_5 on high surface area TiO_2 prepared by impregnation	c	96	0.237	0.199	1.193
5% R					
After catalytic tests		8.9	0.108	0.351	0.308
and consecutive extraction		8.9	0.041	0.401	0.102

area, is equivalent to that necessary to form a complete monolayer on the surface (Table 2).

Tentatively, the broadening of the V^V signal is due to the interaction of vanadium with the titania surface and according to ^{51}V NMR results (*17*) may be interpreted as a change from nearly fivefold to octahedral coordination as a consequence of surface interaction and of coordinatively adsorbed water.

The asymmetric tail, on the contrary, can be interpreted as the overlapping of a small signal of V^{IV} on the main signal of V^V, according also to chemical analysis data (*6*). The deconvolution of the spectra, based on a Gaussian signal for V^{IV} and V^V with a peak position and a FWHM equal to those of V^{IV} in V_2O_4 after long evacuation (*15*) and of V^V in wet impregnated samples (see spectrum *c*) leads to a good fitting of the results. This further confirms the formation of V^{IV} by solid-state reaction of V_2O_5 and TiO_2.

After catalytic tests in *o*-xylene oxidation the analysis of the peak shape reveals a further increase in the V^{IV} content. The position of the V^{IV} peak is slightly shifted to higher binding energies, but it must be noted that in this case a reduced phase of vanadium oxide is formed. In this phase V^{IV} does not interact strongly with the TiO_2 surface, thus this result is different from the previous observation (sample of Fig. 11d). A shift of about 0.3–0.5 eV to higher binding energies may therefore be expected, in agreement with the differences between the spectra of reference compounds such as V_2O_4, $VOCl_2$, and $VOSO_4$ (*6*). In the case of spectrum e, the position of the maximum for the V^{IV} has thus been put equal to that of a V_6O_{13} polycrystalline sample (*15*). Using this value the fitting of the experimental signal is good, indicating the formation of a reduced phase of vanadium oxide during the catalytic tests. Similar results were also obtained for rutile samples.

The depth profile using a Ne^+ ion gun for the sputtering of an anatase sample after catalytic tests (5% A, sample e of Fig. 11) is reported in Fig. 12. The V/O, Ti/O, V/Ti, and O/(V + Ti) atomic ratios are reported as a function of the thickness removed during sputtering. For the analysis of these data it should be considered that, for a mean ki-

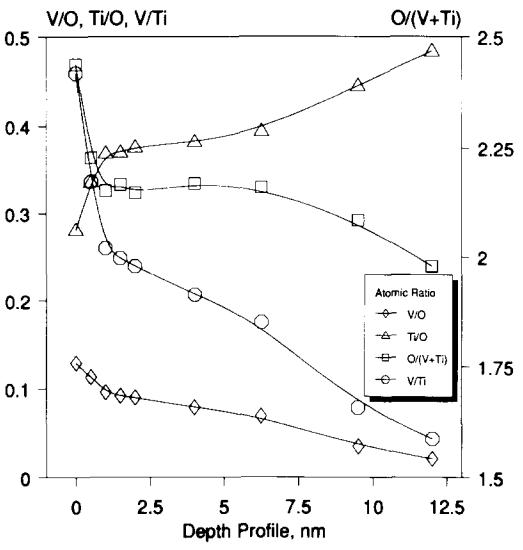

FIG. 12. XPS depth profile of a 5.05% A sample after catalytic tests (at least 500 h of time-on-stream).

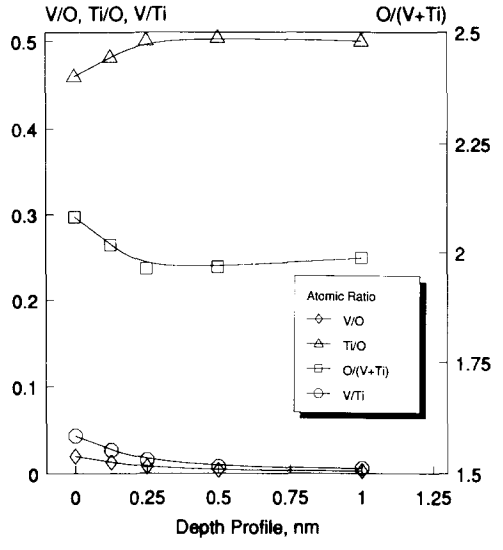

FIG. 13. XPS depth profile of the same sample of Fig. 12 after extraction of the soluble vanadium oxide using a dilute H_2SO_4 solution.

netic energy of 1000 eV, the thickness analyzed by the XPS technique is about 2–3 nm (*27*). The values reported are thus averaged for the surface thickness analyzed, indicating that the absolute value of thickness removed cannot be unambiguously estimated, and also taking into account the error associated with the model of depth profile used and with the sputtering yields of the various elements (see Experimental). Nevertheless, the analysis of the trend of depth profile is indicative of changes in the composition along the particle thickness.

Seen in Fig. 12 is a drastic change in the slope of all atomic ratios after about 1 nm of thickness removed. The V/Ti ratio, for example, decreases from about 0.46 to 0.26 in the first nanometer removed and then decreases slowly almost linearly to around 0.05 in the next 11 nm removed. A corresponding change occurs in the O/(V + Ti) ratio from a value nearly that of V_2O_5 (2.5) to that of TiO_2 (2.0).

The depth profile thus indicates the presence of two phases, one well dispersed on the surface of TiO_2 anatase (mono- or bilayer) and the second phase present as multilayer patches overlying the former phase. An estimated thickness of this multilayer phase, assuming a model of vanadia blocks of different thickness on the titania surface covered with a monolayer of vanadia (*15*), is about 10–15 nm. Both phases are XRD amorphous.

The removal of the soluble part of vanadium by extraction in a dilute sulphuric acid solution (*6*) causes considerable lowering of the V/Ti ratio (Fig. 13). The V/Ti ratio decreases from about 0.05 to nearly 0 after removal of only 0.5 nm of thickness, evidence that after extraction only a single layer of vanadium remains on the surface and no vanadium is present in the bulk of the TiO_2 anatase. The position of the $V_{2p\ 3/2}$ peak is in agreement with the presence of only V^{IV} on the surface of the TiO_2 anatase after extraction, even though the noise to signal ratio as a consequence of the low amount of vanadium does not allow an unequivocal attribution.

In rutile samples after catalytic tests, the two-step depth profile observed for anatase samples (Fig. 12) is no longer present; the V/O and V/Ti atomic ratios decrease almost linearly in a way analogous to that observed

in anatase sample after removal of about 1 nm of thickness. The V/O, Ti/O, and V/Ti atomic ratios in the rutile sample after catalytic tests are, in fact, in agreement with those observed for a mechanical mixture of V_2O_5 and TiO_2 (Table 2). In addition, shown in Table 2 is the higher value of the V/Ti atomic ratio observed in a monolayer VTiO sample prepared by wet impregnation on a high surface area TiO_2 anatase.

Extraction of the soluble part of vanadium in the rutile samples considerably decreases the amount of vanadium detected in the catalyst. However, comparison with the corresponding anatase sample (Table 2), shows the relatively higher amount of residual vanadium. This agrees with the chemical analysis data. Furthermore, the depth profile of vanadium in the sample shows the presence of V throughout the whole bulk phase of TiO_2, in contrast to the results found for anatase samples (Fig. 13).

DISCUSSION

Changes Occurring during o-Xylene Oxidation

Various transformations occur to the solid-state mixture of V_2O_5 and V^{IV}-modified TiO_2 when put in contact with an *o*-xylene/air stream at about 600 K. X-ray diffraction analysis shows the disappearance of the diffraction lines of crystalline V_2O_5 due to the formation of amorphous phases even for amounts of vanadium oxide about 6–7 times higher than that necessary for monolayer coverage. Infrared spectroscopy in the $\nu V{=}O$ region (Fig. 7) shows a shift to lower frequencies (from 1022 to about 995 cm^{-1}) and a broadening of the band. Chemical analysis (Table 1) shows the formation of a partially reduced vanadium-oxide phase with a mean valence state of approximately 4.7 corresponding to a $V^V : V^{IV}$ ratio of about 2 : 1. Solid-state ^{51}V NMR results (Fig. 10) indicate the formation of a main phase characterized by the presence of V^V sites in an octahedral environment analogous to those present in hydrated V-oxide gels (*28*). These indications are in agreement with that deduced from the analysis of the peak shape of the $V_{2p\,3/2}$ signal in the XPS spectra (Fig. 11). All these data on the transformations occurring during *o*-xylene oxidation are roughly similar for both anatase and rutile TiO_2 samples.

Nature of V-Oxide Surface Species after o-Xylene Oxidation

XPS depth profile measurements (Figs. 12, 13, and Table 2) indicate that, in anatase samples, the titania surface is homogeneously covered by a V^{IV}–V^V (partially hydrated and XRD amorphus) mono- or bilayer. When the amount of vanadium exceeds that necessary for the first phase, a second *bulk* phase is also present, whose structural characteristics, however, strongly resemble that of the former phase. The bulk phase is also XRD amorphous and partially reduced ($V^V : V^{IV}$ ratio of about 2). This phase does not homogeneously cover the monolayer phase, but is probably present on the surface as irregular multilayer patches, as suggested by the depth profile.

In rutile samples, the monolayer phase is either not present or is present in much lower amounts; however, islands of partially oxidized V_2O_4 are present together with the same partially reduced vanadium-oxide phase as in the anatase samples. It should be recalled that, in the anatase sample, the whole surface of TiO_2 is modified by non-soluble V^{IV} species as previously discussed (*6*). The V^V sites generated by reduction and amorphization of the crystalline V_2O_5 must thus interact with this V^{IV}-modified surface. ^{51}V NMR data indicate a nearly square-pyramidal coordination and agree with FT–IR and XPS indications of the presence of water in the coordination sphere of V^V.

In addition, it should be noted that a very similar catalytic behavior in *o*-xylene oxidation is observed between supported and unsupported vanadium oxide after attainment of the steady-state behavior. This suggests that the local environment around V^V sites both in the mono- or bilayer and in the over-

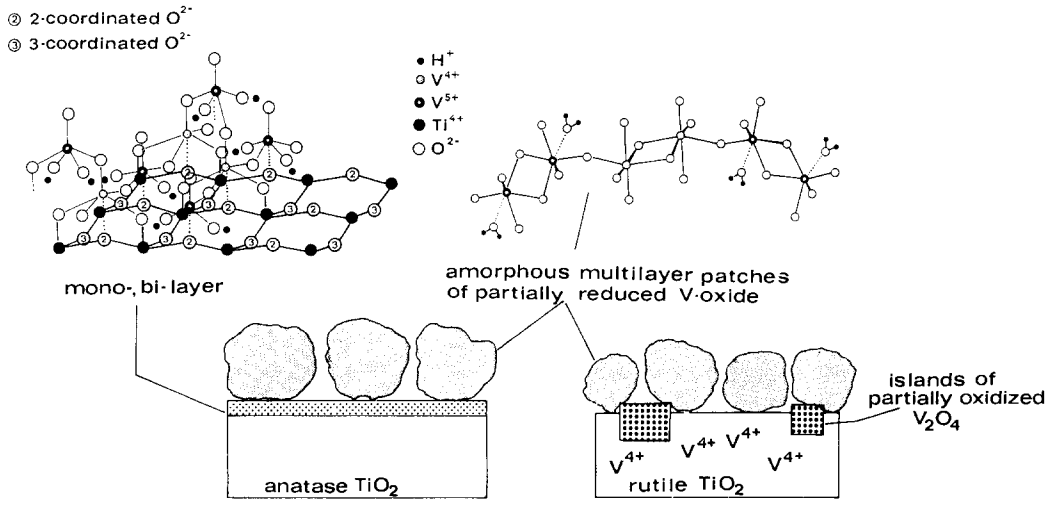

FIG. 14. Model of the surface situation of vanadium-oxide species on TiO_2 anatase or rutile after long-term catalytic tests in samples prepared by solid-state reaction of V_2O_5 and TiO_2 and *in situ* treatments in *o*-xylene oxidation.

laying reduced bulk V-oxide must be relatively similar to that present in a hydrated V_3O_7 phase.

The combination of all these indications with the already discussed model of the surface of TiO_2 (anatase) modified by non-soluble V^{IV} sites and with the idea of a local environment of V^V similar to that of a hydrated V_3O_7 phase, suggests the tentative model reported in Fig. 14 of the mono- or bilayer of V-oxide on the anatase surface. On the basis of the same assumptions and evidence, the model of the overlaying hydrated V_3O_7-like phase could be also formulated (Fig. 14).

Correlation between the Nature of V-Oxide Species and Their Catalytic Behavior

The change in the catalytic behavior when increasing amounts of V_2O_5 were added (Figs. 1 and 2) can be discussed on the basis of the nature of the V-oxide species formed on a TiO_2 surface after *o*-xylene oxidation. It should be noted that the starting compounds are V_2O_5 and V^{IV}-modified TiO_2. The catalytic behavior in *o*-xylene oxidation of the latter phase differs for anatase and rutile samples, as previously discussed (*6*), and shows reactivity higher than that of pure TiO_2.

A continuous increase in the activity (Fig. 1a) and selectivity (Fig. 1b) is observed with increasing amounts of V_2O_5 in anatase samples. In rutile samples the selectivity (at high conversion) and the maximum yield of phthalic anhydride also increase, but the selectivity at low conversion decreases (Fig. 2b). The maximum yield of phthalic anhydride is similar in anatase and rutile samples, but in the latter, the formation of the intermediate phthalide is more important at low conversion.

Two parallel effects occur during the transformation of V_2O_5 during *o*-xylene oxidation, (i) a process of spreading of vanadium in anatase samples with formation of the mono- or bilayer phase and (ii) a process of reduction and amorphization of V_2O_5 crystallites with formation of a partially reduced bulk vanadium-oxide phase overlaying the first phase in the form of irregular multilayer patches. Comparison of the catalytic results for anatase and rutile samples

suggests that the presence of the former phase is not the conditioning factor to obtain selective catalysts for *o*-xylene conversion.

This is confirmed from the catalytic behavior of an unsupported V^{IV}–V^{V} mixed valence sample of vanadium oxide (Fig. 5), the performances of which are comparable in *o*-xylene conversion, apart from the lower specific activity per gram of vanadium oxide. The interaction with the titania support thus favors the activity (number of active sites) more than the selectivity (nature of active sites). This effect, in particular, is reflected in the decrease in formation of the intermediate phthalide which could be assumed as an index of activity. In the more active catalysts the reduced formation of phthalide as well as the lower reaction temperatures leads to a slight increase in selectivity, of the order of 3–4%. This also explains the small difference in the catalytic performances of anatase and rutile based samples (Figs. 1 and 2) in relation to the differences previously discussed on the nature of the monolayer interacting with TiO_2.

In anatase samples, the interaction with the TiO_2-modified surface and the formation of the monolayer lead to a further increase of the specific activity of the active sites with respect to the rutile samples, due to their better dispersion on the catalyst surface.

Furthermore, this enhanced dispersion leads to an increase of the stability against reoxidation of the reduced vanadium-oxide phase in comparison with rutile samples (Figs. 7 and Table 1). This may be interpreted as a consequence of the absence, in the rutile samples, of the well-spread strongly interacting V^{IV} sites which may act as the sites for clinging of the upper phase (*8*).

The difference in stability may be important in the transient evolution as indicated by the slower rate of attainment of the steady-state catalytic behavior in rutile samples in comparison with anatase samples (Figs. 3 and 4). The difference may be important also in the catalytic behavior at the end of the catalytic bed corresponding to the zone of high conversion where the oxygen/*o*-xylene ratio increases considerably. Therefore, this aspect is more critical in industrial reactors where a hot-spot temperature profile is present than in laboratory-scale reactors where the temperature profile is much more uniform.

CONCLUSIONS

The data indicate that the nature of the vanadium-oxide phase is independent of the interaction with the titania support, which principally enhances the number of active sites. The small differences between the performances of the unsupported, the rutile, and anatase catalysts originate from different dispersion of the same active phase. In particular, the anatase samples exhibit the best capability to enhance the dispersion of vanadium with the formation of a mono- or bilayer phase by interaction with a homogeneously V^{IV}-covered TiO_2 surface.

We may remark that the final catalytic behavior of samples prepared by solid-state reaction of V_2O_5 and TiO_2 as well as their physicochemical characterization (especially ^{51}V NMR and FT–IR) indicates the excellent analogy between these catalysts and those obtained by impregnation or grafting techniques. This suggests that these procedures lead to surface vanadium-oxide layer characteristics which before catalytic tests are already similar to that of our catalyst after *o*-xylene oxidation (apart from the mean valence state). Thus in these samples, the rate of transformation in the reaction environment may be higher when put in contact with *o*-xylene/air flow. This explains why the monolayer phase was thought to be the only active/selective phase when only short-term catalytic tests were done and as a consequence V_2O_5 crystallites were thought to be inactive and anatase TiO_2 a much better support than the rutile form (*29–35*). The present data, on the contrary, clearly indicate that V_2O_5 crystallites transform in contact with *o*-xylene/air flow and that the activity/selectivity behavior of this phase is

exactly comparable to that of the monolayer samples (*1–5, 29–36*). Therefore, similar results are obtained using anatase or rutile TiO_2. This result also agrees with the results of Mori *et al.* (*37*) and Niwa *et al.* (*4, 38*). We may also remark that the models of the monolayer normally reported in the literature (*1, 29–34*) do not take into account that this phase is partially reduced during catalytic tests.

With regard to the model presented in Fig. 14, although it is relatively speculative, it takes into account (i) the presence of partially reduced phases after *o*-xylene oxidation, and (ii) of non-soluble V^{IV} species, (iii) the change in the V^{V} coordination environment compared to V_2O_5 and the analogies with the V_3O_7, (iv) the surface structure of V^{IV} species, (v) the indication on the depth profile of vanadium and (vi) of the difference between anatase and rutile TiO_2 samples, and (vii) the analogies in the reactivity between supported or non-supported V-oxide samples.

In conclusion, the model reported in Fig. 14 requires further investigations, but allows a reasonable interpretation of the experimental evidences on the changes in the surface structure of V-oxide on TiO_2 after *o*-xylene oxidation.

REFERENCES

1. Bond, G. C., Flamerz, S., and Shukri, R., *Faraday Discuss. Chem. Soc.* **87,** 65 (1989).
2. Cavani, F., Centi, G., Foresti, E., Trifiró, F., and Busca, G., *J. Chem. Soc. Faraday Trans. 1* **84,** 237 (1988).
3. Andersson, A., and Andersson, S. L. T., *in* "Solid State Chemistry in Catalysis" (R. K. Grasselli and J. F. Brazdil, Eds.), p. 121. ACS Symp. Series 279, American Chemical Society. Washington, DC, 1985.
4. Niwa, M., Matsuoka, Y., and Murakami, Y., *J. Phys. Chem.* **93,** 3660 (1989).
5. Hönicke, D., and Xu, J., *J. Phys. Chem.* **92,** 4699 (1988).
6. Centi, G., Giamello, E., Pinelli, D., and Trifiró, F., *J. Catal.* **129,** 220 (1991).
7. Cavani, F., Foresti, E., Parrinello, F., and Trifiró, F., *Appl. Catal.* **38,** 311 (1988).
8. Centi, G., Pinelli, D., and Trifiró, F., *J. Mol. Catal.* **59,** 221 (1990).
9. Waltersson, K., Forslund, B., Andersson, S., and Galy, J., *Acta Crystallogr. Sect. B* **30,** 2664 (1974).
10. Cavalli, P., Cavani, F., Manenti, I., and Trifiró, F., *Ind. Eng. Chem. Res.* **26,** 639 (1987).
11. Ping-Man, P., Thesis, University of Paris VI, France, 1986.
12. Taouk, B., Thesis, University of Lille, France, 1988.
13. Scofield, J. H., *J. Electron. Spectrosc. Relat. Phenom.* **8,** 129 (1976).
14. Reilman, R. L., Useane, A., and Manson, S. T., *J. Electron. Spectrosc.* **8,** 398 (1976).
15. Mendialdua, J., Thesis, University of Lille, France, 1983.
16. Bachman, H. G., Ahmed, F. R., and Barnes, W. H., *Z. Kristallogr.* **115,** 110 (1965).
17. Echert, H., and Wachs, I. E., *J. Phys. Chem.* **93,** 6796 (1989).
18. Mastikhin, V. M., Lapina, O. B., Krasilnilov, V. N., and Ivakin, A. A., *React. Kinet. Catal. Lett.* **24,** 119 (1984).
19. Lapina, O. B., Simakov, A. V., Mastikhin, V. M., Veniaminov, S. A., and Shubin, A. A., *J. Mol. Catal.* **50,** 55 (1989).
20. Chary, K. V. R., Venkat Rao, V., and Mastikhin, V. M., *J. Chem. Soc. Chem. Commun.*, 202 (1989).
21. Le Costoumer, L. R., Taouk, B., Le Meur, M., Payen, E., Guelton, M., and Grimblot, J., *J. Phys. Chem.* **92,** 1230 (1988).
22. Taouk, B., Guelton, H., Grimblot, J., and Bonnelle, J. P., *J. Phys. Chem.* **92,** 6700 (1988).
23. Gornastansky, S. D., and Stager, C. V., *J. Chem. Phys.* **46,** 4959 (1967).
24. Ragle, J. L., *J. Chem. Phys.* **35,** 753 (1961).
25. Hausinger, G., Schmelz, H., and Knözinger, H., *Appl. Catal.* **39,** 267 (1988).
26. Centi, G., Lena, V., Trifiró, F., Ghoussoub, D., Aïssi, C. F., Guelton, M., and Bonnelle, J. P., *J. Chem. Soc. Faraday* **86** (1990) 2775.
27. Vedrine, J. C., and Jugnet, Y., *in* "Les Techniques Physiques d'etude des Catalyseurs" (B. Imelik and J. C. Vedrine, Eds.), p. 365. Editions Technip, Paris, 1988.
28. Repelin, Y., Husson, E., Abello, L., and Lucazeau, G., *Spectrochim. Acta A* **41,** 993 (1985).
29. Gasior, M., Haber, J., and Machej, T., *Appl. Catal.* **33,** 1 (1987).
30. (**a**) Bond, G. C., and Köning, P., *J. Catal.* **77,** 309 (1982); (**b**) Bond, G. C., *J. Catal.* **116,** 531 (1989).
31. (**a**) Saleh, T. Y., and Wachs, I. E., *Appl. Catal.* **31,** 87 (1987); (**b**) Saleh, R. Y., Wachs, I. E., Chan, S. S., and Chersich, C. C., *J. Catal.* **98,** 102 (1986); (**c**) Saleh, R. Y., Wachs, I. E., Chan, S. S., and Chersich, C. C., *Appl. Catal.* **15,** 339 (1985).
32. Kozlowski, R., Pettifer, R. F., and Thomas, J. M., *J. Phys. Chem.* **87,** 5176 (1983).
33. Kijenski, J., Baiker, A., Glinski, M., Dollenmeier, P., and Wokam, A., *J. Catal.* **110,** 1 (1986).

34. Cristiani, C., Forzatti, P., and Busca, G., *J. Catal.* **116,** 586 (1989).
35. Miyata, H., Fujii, K., One, T., Kubokawa, Y., Ohno, T., and Hatayama, F., *J. Chem. Soc. Faraday Trans. 1* **83,** 675 (1987).
36. Cavani, F., Centi, G., Parrinello, F., and Trifiró, F., *in* "Preparation of Catalysts IV" (B. Delmon, P. Grange, P. A. Jacobs, and G. Poncelet, Eds.), p. 227. Elsevier, Amsterdam, 1987.
37. Mori, K., Miyamoto, A., and Murakami, Y., *J. Chem. Soc. Faraday Trans. 1* **82,** 13 (1986).
38. Niwa, M., Matsuoka, Y., and Murakami, Y., *J. Phys. Chem.* **91,** 4519 (1987).